Distribution Agreement

In presenting this thesis as a partial fulfillment of the requirements for a degree from Emory University, I hereby grant to Emory University and its agents the non-exclusive license to archive, make accessible, and display my thesis in whole or in part in all forms of media, now or hereafter known, including display on the world wide web. I understand that I may select some access restrictions as part of the online submission of this thesis. I retain all ownership to the copyright of the thesis. I also retain the right to use in future works (such as articles or books) all or part of this thesis.

Signature:

_____	_____
Tiffany Petrisko	April 14, 2014

Quantifying Upper Motor Neurons in Rodent Model of Amyotrophic Lateral Sclerosis

by

Tiffany J. Petrisko

Adviser

Nicholas M. Boulis, MD

Neuroscience and Behavioral Biology Program

_____
Nicholas M. Boulis, MD
Adviser

_____
Leah Anderson Roesch, PhD
Committee Member

_____
Shawn Hochman, PhD
Committee Member

_____
4/14/14

Quantifying Upper Motor Neurons in Rodent Model of Amyotrophic Lateral Sclerosis

by

Tiffany Petrisko

Adviser

Nicholas M. Boulis, MD

An abstract of
A thesis submitted to the Faculty of Emory College of Arts and Sciences
of Emory University in partial fulfillment
of the requirements of the degree of
Bachelor of Sciences with Honors

Program in Neuroscience and Behavioral Biology

2014

Abstract

Quantifying Upper Motor Neurons in Rodent Model of Amyotrophic Lateral Sclerosis
By Tiffany J. Petrisko

Amyotrophic Lateral Sclerosis (ALS), more commonly known as Lou Gehrig's disease, is an adult-onset neurodegenerative disorder in which there is a progressive loss of upper (brain) and lower (brainstem and spinal cord) motor neurons. Patients with ALS rapidly lose use of their extremities and become ventilator dependent, with 80% of patients dying within 3-5 years after diagnosis. Animal models have been used over the years to study the mechanisms of this disease as well as a way to test potential therapies. One of the most characterized models involves the over expression of the human SOD1 G93A gene, a mutation known to cause ALS. Currently, there is no data available that shows how the upper motor neurons—specifically rubrospinal and corticospinal motor neurons – compare in SOD1 G93A rats compared to wild-type animals. By injecting a retrograde tracer into the rubrospinal and corticospinal tracts, this study aims to quantify the upper motor neuron count in the red nucleus and motor cortex in both SOD1 G93A and wild-type animals to determine if there is a significant difference. Additionally, the motor neuron counts in the red nucleus will be compared by two methods: the tracer and cresyl violet staining to determine which is more accurate. Results indicate that despite accurate injections in 5 of 10 corticospinal tracts, the tracer did not reach the motor cortex. Rubrospinal tract injections were much less accurate, with only three animals presenting with tracer in the red nucleus. Additional brain areas also expressed tracers, further confirming the inaccuracy of injections. Further investigation with better accuracy, correct timing, and a larger sample size will be able to provide a better understanding of ALS; not only will it further validate the animal model replicating the clinical symptoms of human pathology but also becoming a resource that will allow investigation to determine if potential therapies are improving upper motor neuron survival rather than only behavioral improvements.

Quantifying Upper Motor Neurons in Rodent Model of Amyotrophic Lateral Sclerosis

by

Tiffany Petrisko

Adviser

Nicholas M. Boulis, MD

A thesis submitted to the Faculty of Emory College of Arts and Sciences
of Emory University in partial fulfillment
of the requirements of the degree of
Bachelor of Sciences with Honors

Program in Neuroscience and Behavioral Biology

2014

Table of Contents

Introduction

Amyotrophic Lateral Sclerosis (ALS), more commonly known as Lou Gehrig's disease in the United States, is one of the most common adult-onset neurodegenerative disease with an incidence rate of 1-2/100,000 in most populations (Barber, Mead, & Shaw, 2006). ALS is characterized by the progressive loss of upper motor neurons in the brain as well as lower motor neurons in the spinal cord and brainstem. The loss of upper motor neurons leads patients to experience hypertonia and positive Hoffmann and Babinski signs (Bruijn, Miller, & Cleveland, 2004; Rosler, Truffert, Hess, & Magistris, 2000).

A patient with corticospinal tract damage will exhibit a positive Hoffmann sign (also known as the finger flexor reflex), which can be determined by a neurologist by flicking the patient's middle finger and observing the remaining fingers and thumbs for a reflexive flexion response. A patient with no corticospinal tract damage will show no flexion in the remaining fingers or thumb (T. M. Annaswamy, Sakai, Goetz, Pacheco, & Ozarkar, 2012). A positive Babinski sign in adults (also known as the plantar reflex) which is assessed by applying a stimulus from the patient's heel and curving towards the toes resulting in the toes fanning out rather than curving inwards as in a normal response, is indicative of general upper motor neuron damage (Van Gijn, 1978). The rapid loss of motor neurons leads to 80% of patients dying within 3-5 years after diagnosis, most commonly from loss of cervical neurons that control breathing (Strong, Kesavapany, & Pant, 2005). Currently, the only FDA approved treatment for ALS is the drug riluzole, which, while able to slow the loss of muscle in limbs, is only able to extend patient survival by a few months (Keifer, O'Connor, & Boulis, 2014; Lacomblez, Bensimon, Leigh, Guillet, & Meininger, 1996).

There are two forms of ALS– sporadic (sALS) and familial (fALS). In the sporadic cases, patients have no family history of the disease, whereas in familial cases there is a strong hereditary component. Although familial ALS makes up only a small portion of all ALS cases (5-10%), genetic analysis has revealed several mutations that have allowed scientists to not only understand the molecular mechanisms of the disease, but also create rodent animal models to further both understanding and test potential therapies (Deng et al., 1993; Renton, Chio, & Traynor, 2014; Rosen et al., 1993). The first gene linked to ALS, which was discovered in 1993, was superoxide dismutase 1 (SOD1) and for the next fifteen years was the only known familial mutation and believed to be responsible for 15-20% of all familial ALS cases (Deng et al., 1993; Renton et al., 2014; Rosen et al., 1993). The recent advances in ALS research have revealed a plethora of additional ALS-linked genes, many of which play a role in RNA metabolism and vesicle trafficking. In 2008, two functionally related genes were discovered: TAR DNA-binding protein (TARDBP) and Fused in sarcoma (FUS) (Sreedharan et al., 2008; Vance et al., 2009). TARDBP encodes TBP-43; a major element of ubiquitin positive neuronal inclusions with is hallmark pathology of not only ALS, but also fronto-temporal dementia (FTD) suggesting a connection between these two neurodegernative diseases (Neumann et al., 2006; Sreedharan et al., 2008). Fused in sarcoma (FUS) shares functional homology with TBP-43 (Kwiatkowski et al., 2009; Renton et al., 2014). Mutations in both of these genes are clustered towards RNA-binding domain of the proteins, suggesting disruption in RNA transcription (Renton et al., 2014). Further evidence of a connection between FTD and ALS came with the most recent discovery of a hexanucleotide repeat in C9ORF72 (DeJesus-Hernandez et al., 2011). The expansion repeats accounts for an overwhelming

number of ALS cases: 40% of familial ALS cases and 7% of sporadic cases (DeJesus-Hernandez et al., 2011; Renton et al., 2014). Despite the evidence suggesting C9ORF72 is the most prominent ALS causing mutation, because it has only been discovered in the past three years there is little understanding of the cellular mechanisms underlying the gene's function. Because of its early discovery in 1993, SOD1 remains the most well characterized mutation in cellular function as well as the creation and understanding of animal rodent models (Deng et al., 1994; Deng et al., 1993; Rosen et al., 1993). In normal function, the SOD1 enzyme is responsible for removing free radicals from the body, which, if not removed, can lead to oxidative stress and eventual cell death (Barber et al., 2006; Deng et al., 1993). However, mutant SOD1 does not lead to ALS by a reduction in SOD1 activity but rather by a toxic gain of function, with the exact mechanism remaining elusive (Beckman, Estevez, Crow, & Barbeito, 2001; Bruijn et al., 2004). While there are multiple mutations in the SOD1 gene that lead to ALS, the most studied SOD1 mutation in both mice and rats has been G93A, a missense mutation in which glycine at codon 93 is changed to alanine (Deng et al., 1994; Gurney, 1997, 2000; Howland et al., 2002). Overexpressing mutant human SOD1 has produced transgenic animals that present with similar clinical symptoms to humans, which allows for the study of not only the mechanism of ALS but also potential therapies (Gurney, 1997, 2000; Matsumoto et al., 2006).

Currently, little is known about upper motor neuron degeneration within the rodent models, specifically determining if the degeneration in these models is able to reliably mimic the observed neuron loss in humans. A recent study in mice determined that

degeneration of corticospinal motor neurons and surrounding subcerebral projection neurons occurs presymptomatically and is specific to these cell types – consistent with observed human pathology (Ozdinler et al., 2011). Previous research in the Boulis lab has indicated a trend towards fewer rubrospinal motor neurons, a subset of upper motor neurons, located in the red nucleus in SOD1 rats compared to wild-type rats (unpublished data). If this trend is indeed correct, not only would it provide evidence of similar clinical pathology, but could also allow for translational scientists to have a time course of upper motor neuron degeneration to test the efficacy of potential therapies at increasing upper motor neuron survival at various points in time through the course of the disease.

One problem with determining upper motor neuron counts in rodents is that the number is relatively low. Additionally, the typical protocol for identifying motor neurons in the brain is via morphology, size, and neurotransmitter expression and does not reveal the neurons related to specific motor pathways. In order to focus on the upper motor neurons related directly to these motor pathways, two descending motor tracts were identified for further analysis: the rubrospinal and corticospinal tracts. The rubrospinal tract (RST), which is important in voluntary movement and large muscle movements of the upper extremities, was targeted as it originates in the brain in a very distinct area: the red nucleus (RN). The red nucleus is made up of two parts, the magnocellular red nucleus (RNm) and the parvocellular red nucleus (RNp), with neurons of varying size found in each (Huber et al., 1943; Liang, Paxinos, & Watson, 2012). While the rubrospinal tract is not the main descending motor tract, it has been shown that the tract is able to

compensate when the other descending tracts are damaged (Wang, Smith, & Xu, 2011). Additionally, the corticospinal tract (CST), which originates in the motor cortex and is responsible for voluntary skilled movement was targeted, as it is the main descending motor tract. The corticospinal tract is made up of two separate tracts in the spinal cord: the lateral corticospinal tract and the dorsal corticospinal tract. In the rat, the dorsal corticospinal tract is the more prominent tract (any further reference to the corticospinal tract will be in reference to the dorsal corticospinal tract).

By injecting a retrograde tracer into these two descending motor neuron tracts, any tracer expression will be found only in rubrospinal motor neurons (RSMN) and corticospinal motor neurons (CSMN) respectively. A previous study looked at the red nucleus projections in the mouse by injecting a retrograde tracer into the cervical and lumbar regions of the rubrospinal tract, including rubrospinal neuron counts (Liang et al., 2012). While this experiment gave information about rubrospinal neuron count from the retrograde tracer as well as a comparison to Nissl-stained sections, the study was limited to only wild type mice. A combination of the Ozdinler and Liang studies will be performed to determine if there is any difference in rubrospinal motor neuron and corticospinal motor neuron count in wild type versus $hSOD1^{G93A}$ rats. If successful, determining the upper motor neuron counts in these two regions (red nucleus and motor cortex) at various time points throughout the rat's development could provide insight into when the best time to treat ALS is, as well as if any potential therapies are not only improving rats behaviorally, but if the treatments are capable of improving motor neuron survival. Because the rats will be undergo retrograde injections at 70 days

(presymptomatic) of age but will be perfused at approximately 105 days (symptomatic), it is expected that there will be a significantly fewer CSMN and RSMN in SOD1 versus wild-type rats.

Methods

Animals: Male wild-type (WT) Sprague-Dawley (Charles River Laboratory) and transgenic rats, breeders obtained from Don Cleveland lab (La Jolla, CA) and bred in house, overexpressing the SOD1 gene with a G93A mutation, $hSOD1^{G93A}$ (Howland et al, 2001), were used in this study (n = 5 per group). All animal procedures were approved by the Emory Institutional Animal Care and Use Committee (IACUC) and performed under institutional and national guidelines.

Surgery: The motor neuron tracts were retrogradely labeled via stereotaxic injection of Retro-green Microbeads (Lumaflour) into the cervical (C4-C5) rubrospinal and corticospinal tracts into animals at P70 (Due to time constraints, two SOD1 animals underwent surgery at P55). In order to inject the tracer into the spinal cord, a laminectomy was performed. Animals were anesthetized using 5% isoflurane and maintained on 2% isoflurane throughout surgery and placed in a stereotaxic frame (Stoelting). The hair covering the surgical area was shaved and then cleaned with alternating application of betadine and alcohol. An incision was made directly above the area in which the injection was to occur (C4-C5) through both the skin and muscles until the lamina were reached. A local anesthetic (1% lidocaine) was injected into the surrounding muscles before the paraspinous muscle was retracted and the lamina

removed to reveal the spinal cord. The dura mater was incised with a 27 ½ G needle followed by bilateral injections of Green Retrobeads™ IX (Lumafluor, Cary, NC; 5 µL per injection) into both the rubrospinal and corticospinal tracts using a Hamilton needle gauge. The rubrospinal coordinates were: 1.58 mm off midline and 0.82 mm depth from when syringe first touched midline. Corticospinal coordinates were: 0.1 mm off midline and 1.1 mm depth (Figure 1) (Watson & Dana Reeve, 2009). The needle remained in place for 5 minutes after each injection was completed to minimize backflow. Following suturing, animals received buprenorphine (0.6 ml of 0.015mg/mL subcutaneous) to reduce pain and place in cage on a heating pad until fully awake. Rats were housed in Emory University Division of Animal Resources and allowed water and food *ad libitum.*

Tissue Collection: Animals were sacrificed 5 weeks post surgery. All animals were deeply anesthetized with isoflurane and given an overdose of phenobarbital (Virbac Animal Health; Fortworth, TX) before being transcardially perfused with 4% paraformaldehyde (PFA). The brain and spinal cords were removed and post-fixed in 4% PFA overnight followed by 30% w/v sucrose for 7 days. The brains were initially frozen with dry ice before being frozen to -80 ^{o}C. Brains sectioned rostral to caudal at 40µm using a cryostat (Lecia Biosystems CM 1950; Buffalo Grove, IL) with the first section being mounted directly onto a slide and the following 4 sections placed into one well of a 24-well plate filled with cryoprotectant. The process was repeated until the entire brain was sectioned. The spinal cords were embedded in OCT (Tissue-Tek; Torrance, CA) frozen to -80 ^{o}C and sectioned on a cryostat at 40µm.

Immunocytochemistry: Due to the possible degradation of the microspheres in the presence of glycerol, the slides containing brain sections were mounted thawed at room temperature and washed with PBS before being mounted in Krystalon mounting medium (Harleco; Gibsbstown, NJ). For brain sections containing microspheres, the corresponding free-floating brain sections were mounted after being washed in PBS and allowed to dry overnight. The slides were then stained with Cresyl Violet (Fisher Scientific) for 20 minutes, followed by washes with 95% and 100% ethyl alcohol before being cover-slipped in Permount (Thermo Scientific; Waltham, MA). To ensure that beads were present in the spinal cord, slides were thawed at room temperature and washed with PBS being mounted in Krystalon mounting medium. To ensure injection accuracy, the spinal cords were thawed at room temperature and washed with PBS before underdoing Hemotoxylin and Eosin staining. Slides were stained in hemotoxylin for five minutes and then rinsed under running tap water before being dipped 12 times in Eosin. After 3-4 dips in dH2O to remove extra Eosin, slides were washed with 90% and 100% ethyl alcohol before being mounted in Permount.

Imaging: The upper motor neurons were visualized on a Nikon E400 microscope at multiple magnifications while using the appropriate fluorescent channel. Bright field images were also taken to view cresyl violet stained brain and H&E stained spinal cords. Photomicrographs were taken with a Nikon DS-Fil color digital camera; the images were then analyzed using NIS-Element software (Nikon Instruments, Melville, NY). A neuron was confirmed as an upper motor neuron by having an area of 700 μm^2.

Data Analysis: Student's T-Test was used to determine if there is a significance difference in rubrospinal motor neuron counts when these neurons were identified by the retrograde tracer or by cresyl violet staining.

Results

No Microspheres Present in Motor Cortex

Of the 10 animals injected, no microspheres were found in the motor cortex, suggesting that either 1) a greater length of time was needed for the microspheres to successfully be transported into the motor cortex or 2) poor injection accuracy into the corticospinal tract. Microspheres were present at the injection site of 5 animals. Of those 5 animals, two had microspheres present in the grey matter, suggesting injections were too deep. H&E staining confirmed injection depth was too deep by an average of 0.20 mm. The remaining 3 animals had microspheres present at the injection sites, which were clearly within the corticospinal tract (Figure 2). The average position of Hamilton needle gauge was 0.158 mm over from midline and a depth of 1.02 mm, very close to the determined coordinates of 0.1 mm off the midline and a 1.1 mm depth (Watson & Dana Reeve, 2009).

Microspheres Can Reach Rubrospinal Neurons in the Red Nucleus

Only three of the ten animals injected with microspheres into the rubrospinal tract showed evidence of these microspheres in the corresponding red nucleus. Two of these animals were wild type while only one SOD1 rat showed microspheres in the RN. The microspheres could be found towards the middle of the red nucleus (rostral to caudal);

this was confirmed by the presence of the red nucleus in cresyl violet stained brains preceding and following the brain sections in which microspheres were found. The average of the center of the injection for these three animals was 1.51 mm off the midline and a depth of 0.72 mm (Figure 3). The remaining seven brains had injection tracts more proximal to the center of the cord compared: 1.42 mm off the midline and a depth 0.77 mm. The ideal coordinates for the rubrospinal tract were 1.58 mm off the midline and a 0.82 mm depth (Watson & Dana Reeve, 2009).

Difference in Rubrospinal Motor Neuron Counts between Retrogreen Microspheres and Cresyl Violet Staining

Although there were only three animals to present with microspheres in the red nucleus, a difference was found between the numbers of rubrospinal motor neurons identified by the retrograde tracer and the number identified by cresyl violet staining and visual identification per slide (Figure 4). A T-Test was used to compare the mean motor neuron counts of each slide containing the red nucleus with both methods. In wild-type animals, the difference between these motor neuron counts was not significant ($p = 0.079$; $\mu_1 = 42.5$, $\mu_2 = 59.89$; n=2 animals, 4 brain sections each), but the SOD1 counts did show a significant difference in motor neuron counts per slide with these two difference techniques ($p = 0.019$; $\mu_1 = 42.33$; $\mu_2 = 57.33$; n = 1 animal, 3 brain sections).

Microspheres Present in Additional Brain Regions

While microspheres were only present in the red nucleus of three of the ten animals, microspheres were found in other brain areas in six of the ten animals. These

microspheres were found in were the: oculomotor nucleus (n=4), the periaqueductal grey (n=3), and the dorsal medial hypothalamic nucleus (n=4) (Figure 5).

Discussion

Understanding the time frame of corticospinal motor neuron and rubrospinal motor neuron degeneration in a rodent model of ALS would provide great insight into disease pathology as well as a tool for translational scientists to determine if potential therapies are improving CSMN and RSMN survival. While this study was unable to determine if there is a difference in motor neuron counts between WT and hSOD1^{G93A} animals, it has provided insight into bettering experimental design so that future experiments may succeed.

The lack of microspheres in the motor cortex of the five animals with accurate injection sites in the corticospinal tracts suggest that greater time is needed for the microspheres to travel from the cervical cord to the motor cortex. Previous studies have successfully used red fluorescent microspheres to highlight the corticospinal tract (C4-C6) in mice and these animals were left for a period of ten weeks before being perfused (Ozdinler et al., 2011). In that experiment, the microspheres were used to distinguish between CSMN degeneration and axonal transport deficits, so it is unclear whether or not the 10 week period was due to potential delays in transport due to the corticospinal tract deteriorating in the diseased animals, even though no impairment was found, or if that was the length in time needed for the microspheres to reach the motor cortex of the mice.

The result of microspheres reaching not only the red nucleus but also a number of different brain regions suggests that more accurate targeting of the rubrospinal tract is needed, but that the animals are surviving long enough to ensure that microspheres can be successfully transported to the midbrain. The additional brain areas in which microspheres were found included the oculomotor nucleus, the periaqueductal grey, and the dorsal medial hypothalamic nucleus. The evidence of beads in the dorsal medial hypothalamus suggests that the spinohypothalamic tract, which is responsible – in conjunction of the spinothalamic tract – for transmitting nociceptive information to the brain was injected in stead of the runbrospinal tract (Cliffer, Burstein, & Giesler, 1991; Zhang, Kostarczyk, & Giesler, 1995). The spinohypothalamic tract is located in the lateral finiciulus of the spinal cord, which is located directly below the rubrospinal tract, implying that the injections in these animals were too deep or leakage of the microspheres into surrounding areas occurred (Watson & Dana Reeve, 2009). The presence of microspheres in the both periaqueductal grey and oculomotor nucleus indicates that the spinomesencephalic tract also had uptake of the microspheres. The spinomesencephalic tract, in the dorsal lateral faniculus projects to a multitude of areas; not only the PAG but also the interstitial nucleus of Cajal, nucleus of Darkscchewitsch and Edinger-Westphal nucleus, which are all connected to the oculomotor nucleus (Figure 6) (Watson & Dana Reeve, 2009).

The trend towards a difference in the retrogradely labeled motor neuron count compared to the motor neuron counts obtained by cresyl violet staining in wild-type animals, and an

observed difference in SOD1 animal could indicate several things. Firstly, these results could indicate that not all motor neurons in the red nucleus are part of the rubrospainl tract, resulting in a higher motor neuron count when done only by cresyl violet staining. Alternatively, the result could also indicate that not all axons of the rubrospinal tract were injected with the microspheres and thus unable to transport them to the red nucleus; this hypothesis could also explain the observed results. Additionally, because there was a significant difference in the SOD1 animals, it is also possible that there were problems with retrograde transport due to axonal degeneration. It is also important to note that experimenter was aware whether or not the animals were SOD1 or WT throughout the entire processes. This includes not only the surgery, in which a targeting bias could occur, but also through the imaging and counting process. Even though the experimenter was as objective as possible, it remains probable that a bias occurred when counting the motor neurons with a subconscious bias for a lower motor neuron count in SOD1 animals and/or a higher motor neuron count in the cresyl violet staining compared to the retrograde tracer. This finding of higher motor neuron count in cresyl violet staining compared to the tracer is consistent with previous studies (Liang et al., 2012; Liu, Keefe, Tang, Lin, & Smith, 2014). Because of the low sample number, the statistical data should be taken lightly and as the sample size increases and targeting improves (as well as a blinded study) this result may change.

The next step in this experiment would be to determine the correct survival time to ensure that the microspheres have the necessary time to reach the motor cortex. Since five weeks post injection has been established as too little, various survival time frames seven, nine,

and eleven weeks post injection should be performed in determine the minimum amount of time necessary for the microspheres to be retrogradely transported to the motor cortex.

In regards to the rubrospinal tract, the survival time of five weeks post injection was enough for the microspheres to reach the red nucleus, as evidenced by the presence of microspheres in the red nucleus and other midbrain structures. However, the accuracy of rurbospinal injections must be improved. The rubrospinal tract is a very small target and thus very difficult to accurately inject, as seen by the numerous examples of Retrogreen beads being transported to different midbrain structures. Once targeting has been confirmed in the cervical regions, the experiment could be repeated on a larger sample size of animals. In particular, the animals should undergo surgery within 1-2 days of P70 (rather than a range of P55-P70), to ensure that the motor neuron counts are accurate. Additional ages should be used to determine the time course of both the rubrospinal and corticospinal motor neuron degeneration. Because the tracer would take a minimum of 5 weeks to reach the target areas, it is imperative that the animals are spaced out in age according to when they would be perfused, taking into considering that SOD1 animals reach end-stage at approximately 120 days. Potential days include injections at P30 (presymptomatic) and P90 (symptomatic). Although the use of Flurogold and True Blue retrograde tracers were unsuccessful in the Boulis laboratory, alternative tracers that do not require along time to reach the red nucleus and motor cortex could be used. The use of these tracers would allow for later injection times without fear of the animals reaching endstage before the tracer has reached the targets.

If targeting of the rubrospinal tract is improved along with a correction in post-injection survival time for the corticospinal tract, this study could provide great insight for translational scientists. No only would the study be providing information about when motor neuron degeneration occurs, it would also inform researchers about which method, cresyl violet or retrograde tracing, is the most accurate way to determine this degeneration. The study also has the potential to inform about disease pathology in this animal model of ALS.

References

Annaswamy, T., Irwin, R.W., & Chimes, G.P. (2012). Electrodiagnostic testing before epidural steroid injections. *PM R, 4*(3), 223-229. doi: 10.1016/j.pmrj.2012.02.006

Annaswamy, T.M., Sakai, T., Goetz, L.L., Pacheco, F.M., & Ozarkar, T. (2012). Reliability and repeatability of the hoffmann sign. *PM R, 4*(7), 498-503. doi: 10.1016/j.pmrj.2012.02.019

Barber, S.C., Mead, R.J., & Shaw, P.J. (2006). Oxidative stress in als: A mechanism of neurodegeneration and a therapeutic target. *Biochim Biophys Acta, 1762*(11-12), 1051-1067. doi: 10.1016/j.bbadis.2006.03.008

Beckman, J.S., Estevez, A.G., Crow, J.P., & Barbeito, L. (2001). Superoxide dismutase and the death of motoneurons in als. *Trends Neurosci, 24*(11 Suppl), S15-20.

Bruijn, L.I., Miller, T.M., & Cleveland, D.W. (2004). Unraveling the mechanisms involved in motor neuron degeneration in als. *Annu Rev Neurosci, 27*, 723-749. doi: 10.1146/annurev.neuro.27.070203.144244

Cliffer, K.D., Burstein, R., & Giesler, G.J., Jr. (1991). Distributions of spinothalamic, spinohypothalamic, and spinotelencephalic fibers revealed by anterograde transport of pha-l in rats. *J Neurosci, 11*(3), 852-868.

DeJesus-Hernandez, M., Mackenzie, I.R., Boeve, B.F., Boxer, A.L., Baker, M., Rutherford, N.J., . . . Rademakers, R. (2011). Expanded ggggcc hexanucleotide repeat in noncoding region of c9orf72 causes chromosome 9p-linked ftd and als. *Neuron, 72*(2), 245-256. doi: 10.1016/j.neuron.2011.09.011

Deng, H.X., Gurney, M.E., Pu, H., Chiu, A.Y., Dal Canto, M.C., Polchow, C.Y., . . . et al. (1994). Motor neuron degeneration in mice that express a human cu,zn superoxide dismutase mutation. *Science, 264*(5166), 1772-1775.

Deng, H.X., Hentati, A., Tainer, J.A., Iqbal, Z., Cayabyab, A., Hung, W.Y., . . . et al. (1993). Amyotrophic lateral sclerosis and structural defects in cu,zn superoxide dismutase. *Science, 261*(5124), 1047-1051.

Gurney, M.E. (1997). The use of transgenic mouse models of amyotrophic lateral sclerosis in preclinical drug studies. *J Neurol Sci, 152 Suppl 1*, S67-73.

Gurney, M.E. (2000). What transgenic mice tell us about neurodegenerative disease. *Bioessays, 22*(3), 297-304. doi: 10.1002/(SICI)1521-1878(200003)22:3<297::AID-BIES12>3.0.CO;2-I

Howland, D.S., Liu, J., She, Y., Goad, B., Maragakis, N.J., Kim, B., . . . Rothstein, J.D. (2002). Focal loss of the glutamate transporter eaat2 in a transgenic rat model of sod1 mutant-mediated amyotrophic lateral sclerosis (als). *Proc Natl Acad Sci U S A, 99*(3), 1604-1609. doi: 10.1073/pnas.032539299

Huber, G.C., Crosby, E.C., Woodburne, R.T., Gililan, L.A., Brown, L.O., & Tamathi, B. (1943). The mammalian midbrain and isthmus regions. Part i: The nuclear pattern. *J Comp Neurol, 78*, 129-534.

Keifer, O.P., Jr., O'Connor, D.M., & Boulis, N.M. (2014). Gene and protein therapies utilizing vegf for als. *Pharmacol Ther, 141*(3), 261-271. doi: 10.1016/j.pharmthera.2013.10.009

Kwiatkowski, T.J., Jr., Bosco, D.A., Leclerc, A.L., Tamrazian, E., Vanderburg, C.R., Russ, C., . . . Brown, R.H., Jr. (2009). Mutations in the fus/tls gene on

chromosome 16 cause familial amyotrophic lateral sclerosis. *Science, 323*(5918), 1205-1208. doi: 10.1126/science.1166066

Lacomblez, L., Bensimon, G., Leigh, P.N., Guillet, P., & Meininger, V. (1996). Dose-ranging study of riluzole in amyotrophic lateral sclerosis. Amyotrophic lateral sclerosis/riluzole study group ii. *Lancet, 347*(9013), 1425-1431.

Liang, H., Paxinos, G., & Watson, C. (2012). The red nucleus and the rubrospinal projection in the mouse. *Brain Struct Funct, 217*(2), 221-232. doi: 10.1007/s00429-011-0348-3

Liu, Y., Keefe, K., Tang, X., Lin, S., & Smith, G.M. (2014). Use of self-complementary adeno-associated virus serotype 2 as a tracer for labeling axons: Implications for axon regeneration. *PLoS One, 9*(2), e87447. doi: 10.1371/journal.pone.0087447

Matsumoto, A., Okada, Y., Nakamichi, M., Nakamura, M., Toyama, Y., Sobue, G., . . . Okano, H. (2006). Disease progression of human sod1 (g93a) transgenic als model rats. *J Neurosci Res, 83*(1), 119-133. doi: 10.1002/jnr.20708

Neumann, M., Sampathu, D.M., Kwong, L.K., Truax, A.C., Micsenyi, M.C., Chou, T.T., . . . Lee, V.M. (2006). Ubiquitinated tdp-43 in frontotemporal lobar degeneration and amyotrophic lateral sclerosis. *Science, 314*(5796), 130-133. doi: 10.1126/science.1134108

Ozdinler, P.H., Benn, S., Yamamoto, T.H., Guzel, M., Brown, R.H., Jr., & Macklis, J.D. (2011). Corticospinal motor neurons and related subcerebral projection neurons undergo early and specific neurodegeneration in hsod1g(9)(3)a transgenic als mice. *J Neurosci, 31*(11), 4166-4177. doi: 10.1523/JNEUROSCI.4184-10.2011

Renton, A.E., Chio, A., & Traynor, B.J. (2014). State of play in amyotrophic lateral sclerosis genetics. *Nat Neurosci, 17*(1), 17-23. doi: 10.1038/nn.3584

Rosen, D.R., Siddique, T., Patterson, D., Figlewicz, D.A., Sapp, P., Hentati, A., . . . et al. (1993). Mutations in cu/zn superoxide dismutase gene are associated with familial amyotrophic lateral sclerosis. *Nature, 362*(6415), 59-62. doi: 10.1038/362059a0

Rosler, K.M., Truffert, A., Hess, C.W., & Magistris, M.R. (2000). Quantification of upper motor neuron loss in amyotrophic lateral sclerosis. *Clin Neurophysiol, 111*(12), 2208-2218.

Sreedharan, J., Blair, I.P., Tripathi, V.B., Hu, X., Vance, C., Rogelj, B., . . . Shaw, C.E. (2008). Tdp-43 mutations in familial and sporadic amyotrophic lateral sclerosis. *Science, 319*(5870), 1668-1672. doi: 10.1126/science.1154584

Strong, M.J., Kesavapany, S., & Pant, H.C. (2005). The pathobiology of amyotrophic lateral sclerosis: A proteinopathy? *J Neuropathol Exp Neurol, 64*(8), 649-664.

Van Gijn, J. (1978). The babinski sign and the pyramidal syndrome. *J Neurol Neurosurg Psychiatry, 41*(10), 865-873.

Vance, C., Rogelj, B., Hortobagyi, T., De Vos, K.J., Nishimura, A.L., Sreedharan, J., . . . Shaw, C.E. (2009). Mutations in fus, an rna processing protein, cause familial amyotrophic lateral sclerosis type 6. *Science, 323*(5918), 1208-1211. doi: 10.1126/science.1165942

Wang, X., Smith, G.M., & Xu, X.M. (2011). Preferential and bidirectional labeling of the rubrospinal tract with adenovirus-gfp for monitoring normal and injured axons. *J Neurotrauma, 28*(4), 635-647. doi: 10.1089/neu.2010.1566

Watson, C.P.G.K.G.C., & Dana Reeve, F. (2009). The spinal cord a christopher and dana reeve foundation text and atlas. from http://www.sciencedirect.com/science/book/9780123742476

Zhang, X., Kostarczyk, E., & Giesler, G.J., Jr. (1995). Spinohypothalamic tract neurons in the cervical enlargement of rats: Descending axons in the ipsilateral brain. *J Neurosci, 15*(12), 8393-8407.

Figures

Figure 1: Schematic of the Rubrospinal and Corticospinal Tracts and the Location of the Red Nucleus in the Brain
A. The rubrospinal tract, which begins in the red nucleus and continues down the spinal cord. **B.** The corticospinal tract, which beings in the motor cortex, crosses in the medulla oblongata, and continues down the spinal cord. **C.** Cross section schematic of the cervical spinal cord showing the location and injection coordinates of the rubrospinal tract (RST) and corticospinal tracts (CST). **D.** Location of the red nucleus in the midbrain of a wild-type rat.

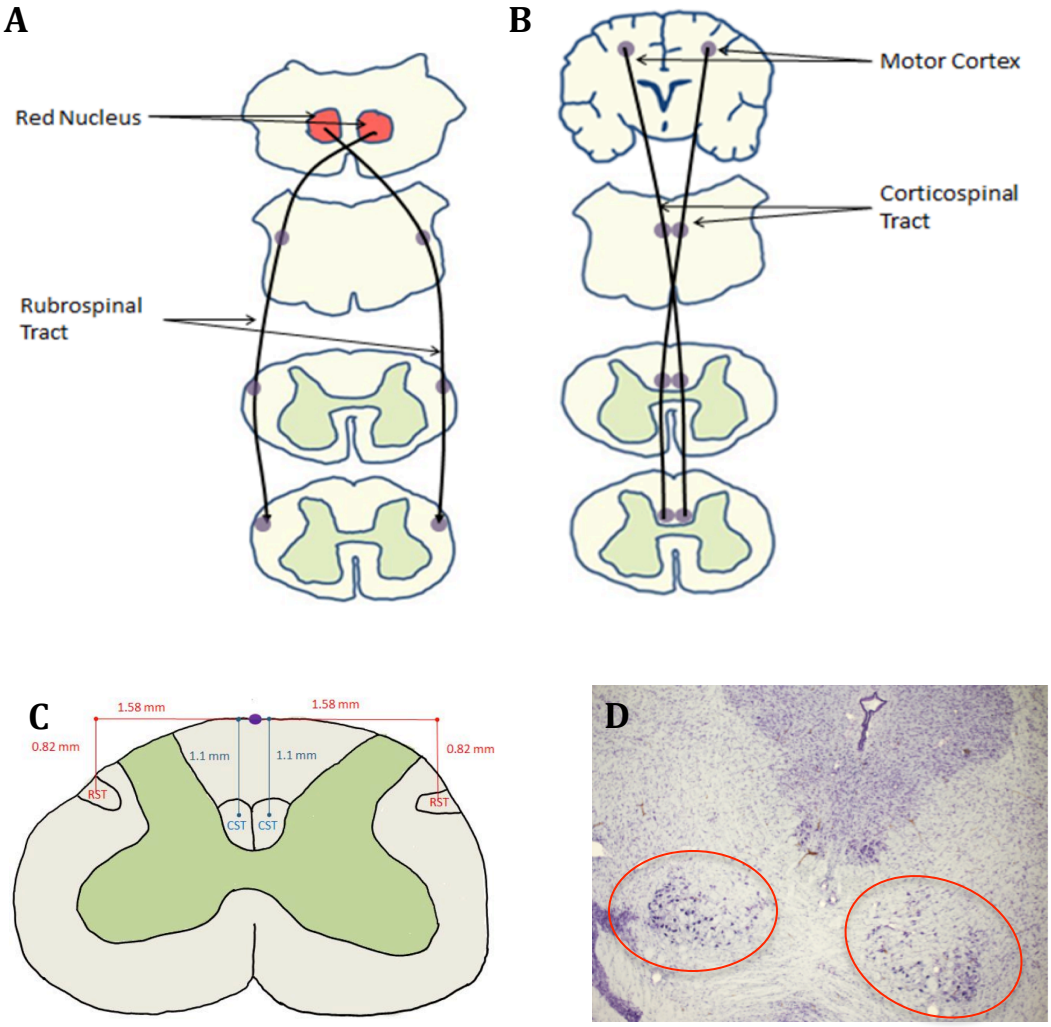

Figure 2: Accuracy of Corticospinal Tract Injections
A. Presence of microspheres in an accurate CST injection (4X). **B.** Corresponding H&E stained section of spinal cord with injection coordinates (4X). **C.** Presence of microspheres in an inaccurate CST injection (4X). **D.** Corresponding H&E stained section of spinal cord with injection coordinates (4X). Red lines indicate injection tract.

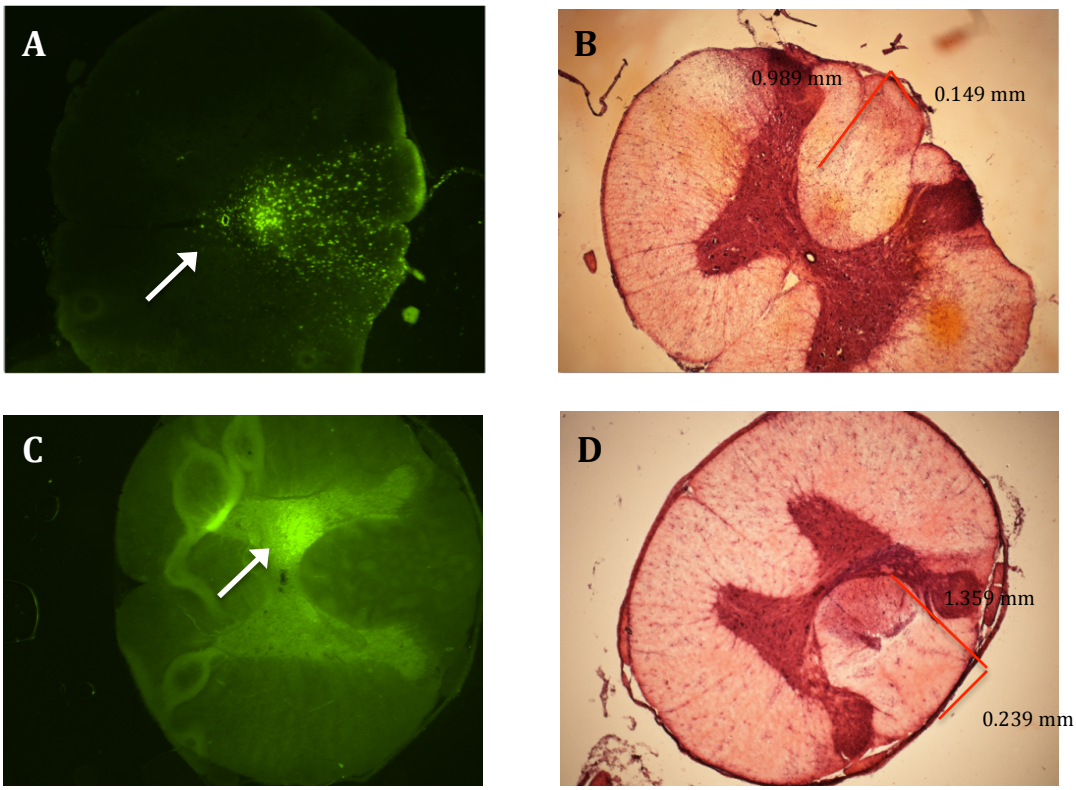

Figure 3: Accuracy of Rubrospinal Tract Injections
A. Presence of microspheres in an accurate RST injection (4X). **B.** Corresponding H&E stained section of spinal cord with injection coordinates (4X). **C.** Presence of microspheres in an inaccurate RST injection (4X). **D.** Corresponding H&E stained section of spinal cord with injection coordinates (4X). Red lines indicate injection tract.

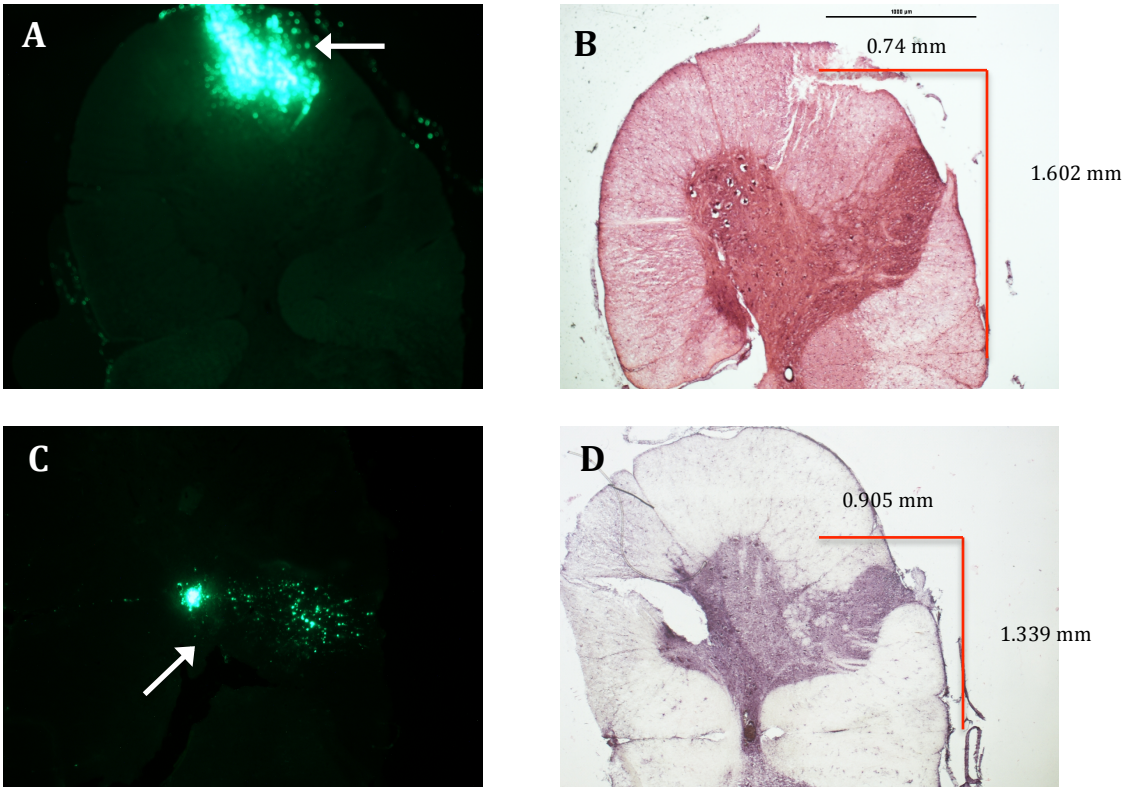

Figure 4: Comparison of Rubrospinal Motor Neuron Counts by Retrogreen Microspheres and Cresyl Violet Staining
A. Presence of microspheres in the red nucleus (boxed area) (4X). **B.** Enlargement of (A), with arrows indicating motor neurons expressing the microspheres (10X). **C.** Corresponding brain section to (B), stained with cresyl violet, showing the location of the red nucleus (boxed area). **D.** Graph showing the average number of motor neurons in the red nucleus per section in both WT and SOD1 animals

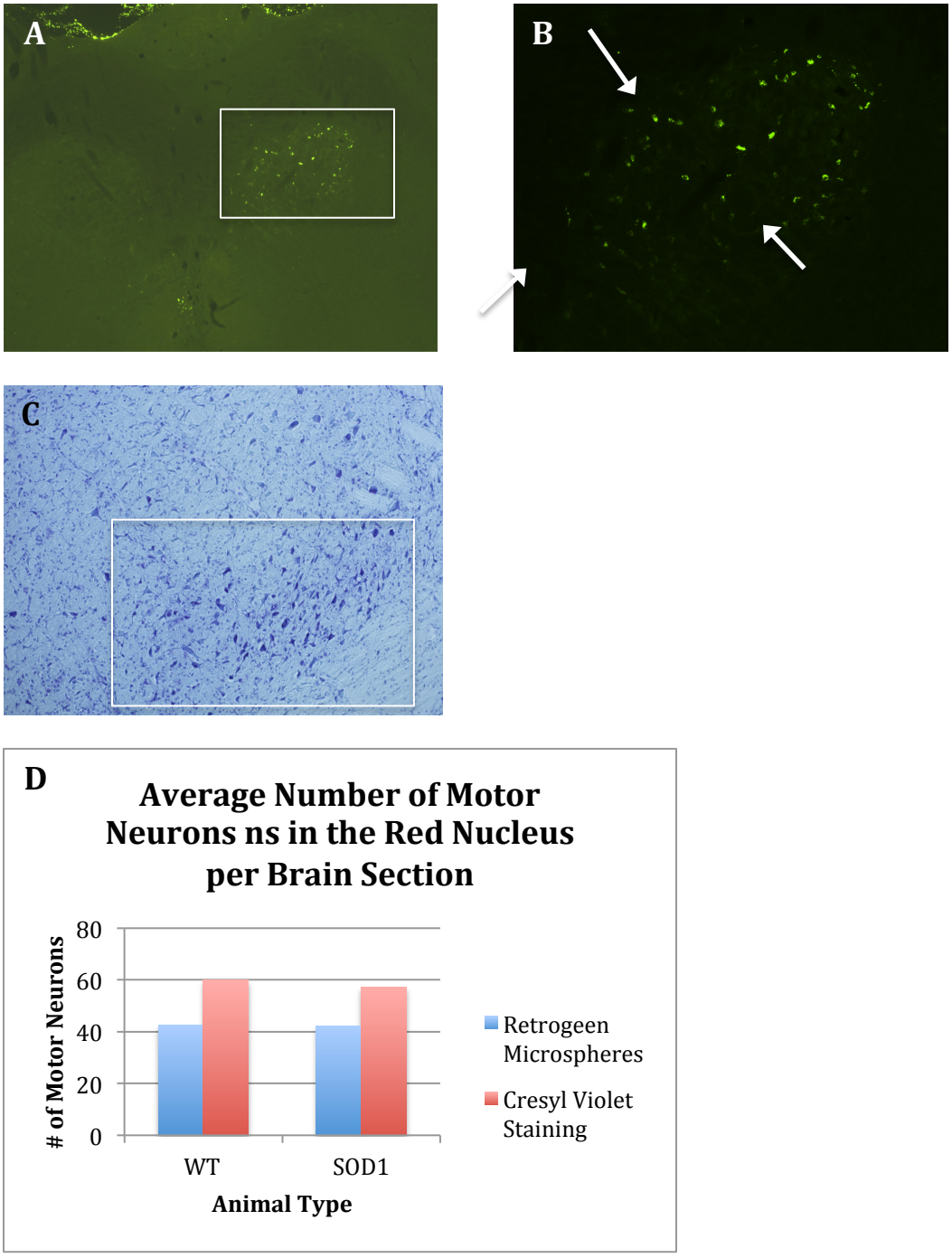

Figure 5: Retrogreen Microspheres Present in Additional Brain Regions
A. Microspheres present in the periaqueductal grey (10X). **B.** Microspheres present in the dorsal medial hypothalamus (10X). **C.** Microspheres present in the oculomotor cortex (10X). Arrows indicate motor presence of microspheres

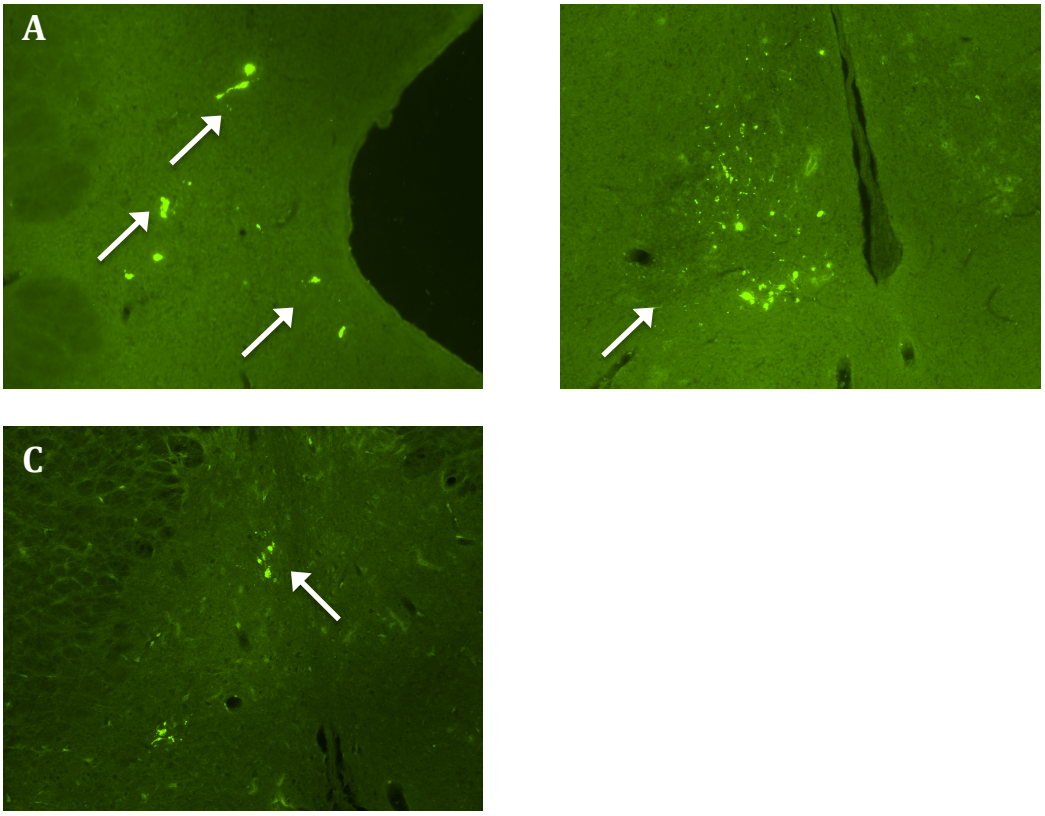

Figure 6: Cross-Sectional Schematic of Spinal Cord Indicating Location of Additional Spinal Tracts also Injected
A. Red lines indicate additional areas of the spinal cord in which axons could have also taken up the microspheres. The spinohypothalamic tract located in the lateral finiculus and the spinomesencephalic tract located in the dorsal lateral finiculus located

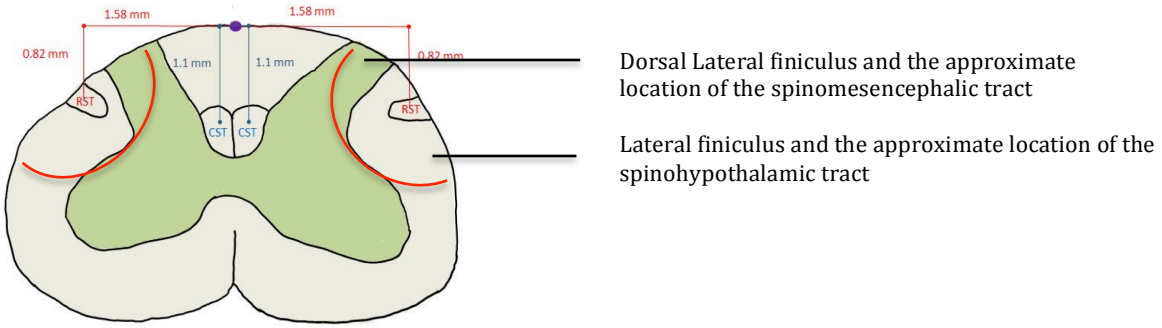

Appendix A

Abbreviations

Name	Abbreviation
Amyotrophic Lateral Sclerosis	ALS
Sporadic Amyotrophic Lateral Sclerosis	sALS
Familial Amyotrophic Lateral Sclerosis	fALS
Superoxide Dismutase 1	SOD1
TAR DNA Binding Protein	TARDBP
Fused in Sarcoma	FUS
Fronto-temporal Dementia	FTD
Rubrospinal Tract	RST
Red Nucleus	RN
Magnocellular Red Nucleus	RNm
Parvocellular red Nucleus	RNp
Corticospinal Motor Neuron	CST
Rubrospinal Motor Neuron	RSMN
Corticospinal Motor Neuron	CSMN